# Permeability and Ferromagnetic Resonance Study for Magnetic Nanowires Substrate With Copper Layer

Yali Zhang<sup>®</sup>, *Graduate Student Member, IEEE*, Joseph Um<sup>®</sup>, *Member, IEEE*, Bethanie Stadler<sup>®</sup>, *Senior Member, IEEE*, and Rhonda Franklin, *Senior Member, IEEE* 

Abstract—In this letter, a straightforward accurate method for magnetic nanowires (MNWs) ferromagnetic resonance (FMR) frequency determination and permeability extraction is proposed. FMR frequencies are obtained using a one-port coplanar waveguide (CPW) circuit system. Relative permeability, defined as  $\mu = \mu' - j\mu''$ , of MNW samples is extracted by "four steps" method, commonly used for thin films (Bekker et al., 2004; Liu et al., 2005; Wei et al., 2015). MNW samples with and without copper (Cu) layer are compared. Samples with a Cu layer show stronger FMR resonances, negligible influences from board resonances, and low distortion  $\mu'$  compared to those without a Cu layer. From  $\mu''$ , the average linewidth of a cobalt sample with and without Cu layer is 4.96 and 5.6 GHz, respectively. From the peak of  $\mu''$ , the FMR frequency of an iron sample is higher at low dc field when compared to cobalt. This can be beneficial for microwave device design when external dc field is limited, and higher operating frequency is required.

Index Terms—Coplanar waveguide (CPW), ferromagnetic resonance (FMR), magnetic nanowires (MNWs), vector network analyzer (VNA).

### I. INTRODUCTION

AGNETIC nanowires (MNWs) are attracting broad interest in microwave device design in transmitting and receiving modules for wireless communication technology [4]–[6]. Their long thin shape provides high shape anisotropy along the wire axis, which creates a large remnant state. This feature allows MNWs to possess gigahertz frequency range ferromagnetic resonance (FMR) absorption at low dc fields and to eliminate the need for an external magnet when applied in nonreciprocal microwave devices. Therefore, MNW-based microwave devices are desirable for future wireless communication. Also, MNWs are grown in a porous anodized aluminum oxide (AAO) template that provides high compactness and stability. Examples of recent designs based on MNWs include circulators [7], band-stop filters [8], and isolators [9].

Manuscript received August 6, 2020; accepted September 3, 2020. This work was supported by the National Science Foundation (NSF) under Award ECCS 1509543 and roll-imprint manufacturing of three-dimensional nanomagnetic arrays CMMI 1762884 with portions conducted in the Minnesota Nano Center which is supported by the NSF National Nano Coordinated Infrastructure Network under Award ECCS-2025124. (Corresponding author: Yali Zhang.)

The authors are with the Department of Electrical and Computer Engineering, University of Minnesota, Minneapolis, MN 55455 USA (e-mail: zhan4898@umn.edu; umxxx023@umn.edu; stadler@umn.edu; rfrank01@umn.edu).

Color versions of one or more of the figures in this letter are available online at http://ieeexplore.ieee.org.

Digital Object Identifier 10.1109/LMWC.2020.3025490

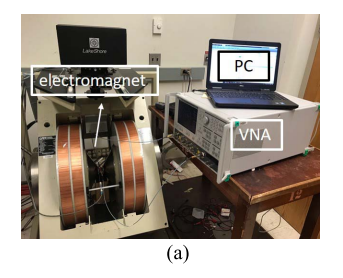




Fig. 1. (a) VNA-FMR system. (b) One-port CPW with MNW sample above.

To design microwave devices in a full-wave modeling tool, the permeability of MNW that has an orientation dependence is needed and is not readily available in software like CST and HFSS. Therefore, a method to characterize the FMR properties of MNWs and extract their relative permeability is needed and required to accurately model circuits using this material.

Herein is a method to obtain FMR frequencies of MNWs and their permeability. It uses a vector network analyzer (VNA)-FMR system [10] based on a one-port coplanar waveguide (CPW) circuit that is connected to a VNA. The "four steps" method [1]–[3] commonly used for thin films is applied to extract the relative permeability. Compared to thin films, MNWs possess much weaker FMR signal strength, and therefore, it is more difficult to extract permeability values accurately. Thus, a copper (Cu) layer is deposited on the back of MNW samples to enhance the FMR signal strength. The FMR responses of a cobalt (Co) sample with and without Cu backing layer are shown. The results are compared to determine the signal enhancement effects due to the Cu layer. Next, a comparison between FMR frequencies and the Kittel equation [11] is shown to confirm the accuracy. Finally, the permeability is extracted for a Co with and without the Cu layer and only for an iron (Fe) MNW sample with the Cu layer.

## II. SYSTEM SET-UP AND SAMPLE DESCRIPTION

The characterization system shown in Fig. 1(a) contains a one-port CPW circuit, an MNW sample, two poles from an electromagnet, and an Anritsu 37369D VNA. The MNW sample is placed above the CPW that is connected to the VNA. The VNA provides an ac field that is swept in the range 0.04–40 GHz and detects FMR response by reflection coefficient ( $S_{11}$ ). The CPW circuit with an MNW sample is then put between two poles from electromagnet that provides a constant dc magnetic field in the range 0–0.55 T.

1531-1309 © 2020 IEEE. Personal use is permitted, but republication/redistribution requires IEEE permission. See https://www.ieee.org/publications/rights/index.html for more information.

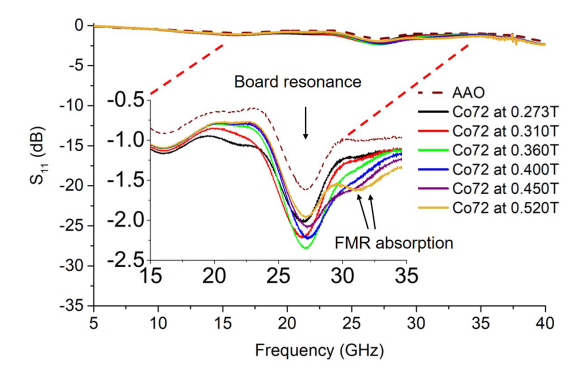


Fig. 2. Reflection response  $(S_{11})$  versus frequency for MNW sample and empty AAO placed on top of the CPW circuit. The Co72 without Cu and AAO samples are evaluated at different dc field values to identify board resonances and FMR absorption peaks.

CPW circuits are designed on a 0.254-mm 5880LZ Duroid ( $\varepsilon_r = 2$ ) with a signal linewidth of 391  $\mu$ m and a slot width of 150  $\mu$ m [Fig. 1(b)]. All measurements have been taken in out-of-plane (OP) orientation, defined as the dc field applied along the wire axis.

MNW samples are grown inside a 50- $\mu$ m-thick AAO template by electrodeposition method [12]. One Co sample, Co72, and one Fe sample, Fe47, are used. Co sample has no crystalline anisotropy. Co72 and Fe47 have an nanowire (NW) length of 15.5 and 10.5  $\mu$ m, respectively. Both have an NW diameter of 40 nm and a porosity of 12% (tolerance:  $\pm 3\%$ ). A 7-nm Ti layer and a 300-nm Cu layer are deposited at the back of MNW samples. Both samples are diced into chips with a chip length of 3 mm and a chip width of 2 mm.

By hysteresis loop measurements, the shape anisotropy, defined as the differences between saturation field along with and perpendicular to the wire axis, obtained for Co72 and Fe47 are 4446 and 8270 Oe, respectively.

#### III. MEASUREMENT RESULTS AND ANALYSIS

# A. FMR Resonance Study

Fig. 2 shows the S<sub>11</sub> response of AAO and Co72 without the Cu layer on the CPW circuit. The AAO template is used to provide a reference. Co72 MNWs grown inside AAO is measured at different dc fields. Board resonances and FMR responses are identified. A board resonance for AAO above CPW is observed around 27.2 GHz. The FMR resonances of Co72 can be observed at 0.45 and 0.52 T when they are located away from the board resonances. Below 0.4 T, FMR resonances overlap with board resonances and are hard to determine. To resolve this issue, a Cu layer has been deposited on one side of the Co72 sample to enhance the FMR signal, as shown in Fig. 3. The presence of the Cu layer attracts the magnetic fields from the slots of CPW to the region above the signal line as shown in [13] to enhance the FMR absorption.

In Fig. 3, the FMR absorptions of Co72 with the Cu layer can be clearly observed at all five different dc fields. The FMR signal strengths are around -4 dB and stronger compared to Co72 without Cu layer, which are around -1.6 dB. When the Cu backing layer is included, however, three parasitic resonances are introduced at 12, 17.5, and around 37 GHz. These resonances are related to the capacitance introduced between Cu layer and CPW circuit and inductance of MNWs.

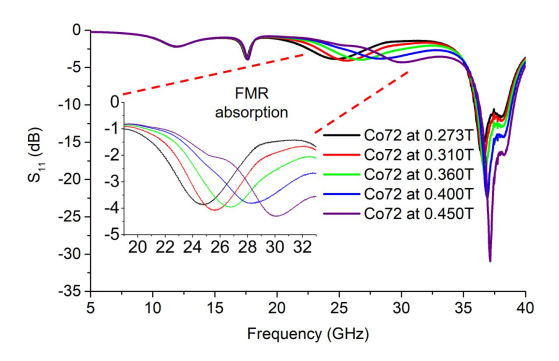


Fig. 3. S<sub>11</sub> response of Co72 with Cu backing layer at different dc fields.

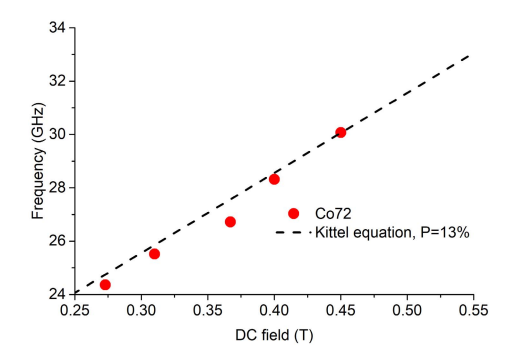


Fig. 4. FMR comparison between Co72 and the Kittel equation.

Therefore, while the Cu layer offers signal enhancement benefits that result in higher FMR absorption and ease of detection, it can also introduce unwanted parasitic resonances in the frequency domain. In this work, however, these parasitic resonant frequencies do not interfere with the FMR frequencies of interest. The factors that control the frequency and signal strength of parasitic resonances are being investigated.

To confirm the accuracy of FMR frequency extraction, FMR frequencies of Co72 with Cu layer are compared to the Kittel equation [11] as shown in Fig. 4. The Kittel equation in OP orientation [14] is described as

$$\frac{f_R}{\gamma} = H + 2\pi M_s - 6\pi M_s P \tag{1}$$

where  $f_R$  is the FMR resonances,  $\gamma$  is the gyromagnetic ratio value of 3.003 MHz/Oe for Co sample, H is the external dc field, P is the porosity of MNW sample, and  $M_s$  is the saturation magnetization with 1440 emu/cm<sup>3</sup> for Co.

Fig. 4 shows that FMR frequencies of Co72 align well with the Kittel equation at P=13%. Since the porosity of Co72 is 12% with  $\pm 3\%$  tolerance, the measured porosity is within the range and the accuracy of measured FMR frequencies can be confirmed.

# B. Permeability Extraction

The relative permeability is extracted based on the "four steps" method [1]–[3]. Considering CPW structure, permeability includes two components contributed by ac fields above the signal line and slots. One study shows that FMR absorption comes from the orthogonality of the ac field and magnetization [15]. Herein, measurements are taken in OP orientation. Therefore, only ac fields above the signal line contribute to the extracted permeability since the ac signal and dc magnetization above the slot are primarily parallel.

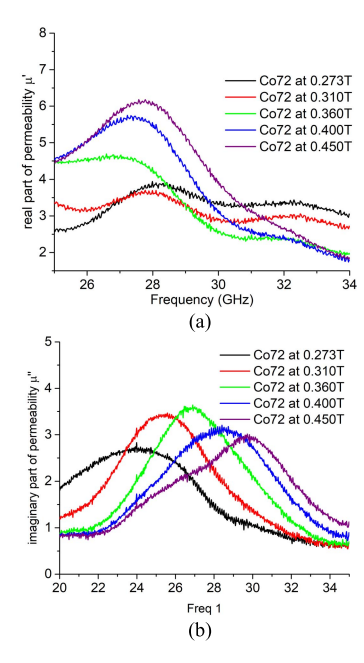


Fig. 5. Permeability of Co72 without Cu layer. (a) Real part of permeability  $\mu'$ . (b) Imaginary part of permeability  $\mu''$ .

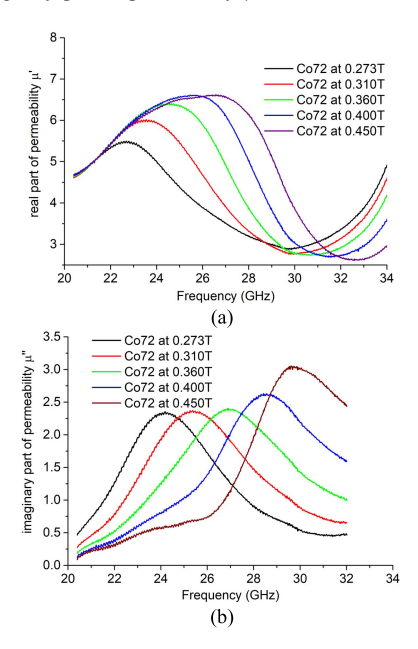


Fig. 6. Permeability of Co72 with Cu layer. (a) Real part of permeability  $\mu'$ . (b) Imaginary part of permeability  $\mu''$ .

The extracted permeability of Co72 without the Cu layer is shown in Fig. 5. The real part of permeability ( $\mu'$ ) for dc fields below 0.36 T, shown in Fig. 5(a), is influenced by the board resonance and distorted from 25 to 29.5 GHz. The imaginary parts ( $\mu''$ ) show less influence from the board resonance. The average linewidth is obtained by calculating the average of full-width at half-maximum of all  $\mu''$  curves. The calculated linewidth of Co72 without the Cu layer is 5.6 GHz.

In Fig. 6,  $\mu'$  and  $\mu''$  of Co72 with Cu layer are shown. The real part of permeability ( $\mu'$ ) in Fig. 6(a) has less distortion from the board resonance, which is more accurate, compared to Co72 without the Cu layer [Fig. 5(a)]. This is due to stronger FMR absorption resulting from the Cu backing layer. The average linewidth of Co72 with the Cu layer is 4.96 GHz and is 11% smaller than the sample without the Cu layer.

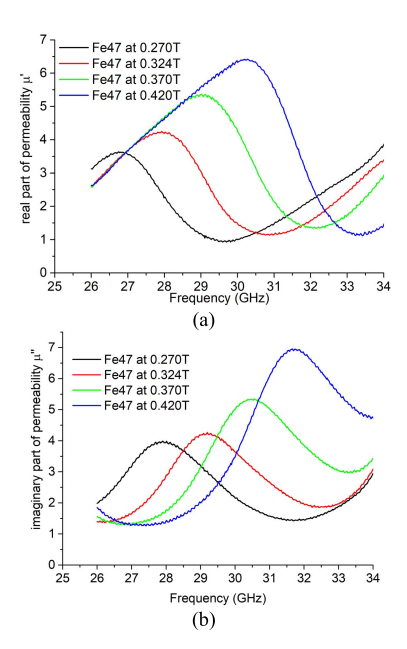


Fig. 7. Permeability of Fe47 with Cu layer. (a) Real part of permeability  $\mu'$ . (b) Imaginary part of permeability  $\mu''$ .

This shows the potential of Cu backing layer to decrease the linewidth of the material which relates to the damping loss. The peak values of  $\mu''$  indicate the FMR frequencies which agree with the FMR frequencies in Fig. 3.

The extracted relative permeability of Fe47 with the Cu backing layer is shown in Fig. 7. Compared to Co samples, Fe MNWs possess higher FMR frequencies at a low dc field due to higher saturation magnetization. For example, the FMR is 31.86 GHz for Fe47 at 0.42 T [Fig. 7(b)] and is 30.07 GHz for Co72 at 0.45 T [Fig. 6(b)]. This feature can be beneficial for microwave device design when the external dc field is limited but the higher operating frequency is required.

# IV. CONCLUSION

In this work, an FMR and permeability study have been implemented for MNWs substrate based on a one-port CPW system in the frequency domain. The FMR frequencies of Co72 MNW samples have been measured and compared to the Kittel equation. A comparison of signal strength for MNWs in Co shows signal enhancement due to the Cu layer. The permeability of Co and Fe samples was extracted based on the "four steps" method. Extracted  $\mu'$  of Co72 with Cu layer performs as expected due to higher signal intensity and has negligible board resonance influences compared to Co72 without Cu layer that experience distortion. Therefore, the deposited Cu layer makes determining the FMR response and extracting the permeability easier and more accurate. Finally, the extracted permeability of Fe47 compared to Co72 shows higher FMR frequencies. This feature can be beneficial for microwave device design when the external dc field is limited, and higher operating frequency is required. In conclusion, this letter presents a straightforward and accurate way to extract required design parameters, FMR frequencies, linewidth, and permeability needed for microwave devices design.

#### REFERENCES

[1] V. Bekker, K. Seemann, and H. Leiste, "A new strip line broad-band measurement evaluation for determining the complex permeability of thin ferromagnetic films," *J. Magn. Magn. Mater.*, vol. 270, no. 3, pp. 327–332, Apr. 2004.

- [2] Y. Liu, L. Chen, C. Y. Tan, H. J. Liu, and C. K. Ong, "Broadband complex permeability characterization of magnetic thin films using shorted microstrip transmission-line perturbation," *Rev. Sci. Instrum.*, vol. 76, no. 6, Jun. 2005, Art. no. 063911.
- [3] J. Wei, H. Feng, Z. Zhu, Q. Liu, and J. Wang, "A short-circuited coplanar waveguide to measure the permeability of magnetic thin films: Comparison with short-circuited microstrip line," *Rev. Sci. Instrum.*, vol. 86, no. 11, Nov. 2015, Art. no. 114705.
- [4] G. Hamoir, J. De La Torre Medina, L. Piraux, and I. Huynen, "Self-biased nonreciprocal microstrip phase shifter on magnetic nanowired substrate suitable for gyrator applications," *IEEE Trans. Microw. Theory Techn.*, vol. 60, no. 7, pp. 2152–2157, Jul. 2012.
- [5] G. Hamoir, L. Piraux, and I. Huynen, "Control of microwave circulation using unbiased ferromagnetic nanowires arrays," *IEEE Trans. Magn.*, vol. 49, no. 7, pp. 4261–4264, Jul. 2013.
- [6] B. K. Kuanr, V. Veerakumar, R. Marson, S. R. Mishra, R. E. Camley, and Z. Celinski, "Nonreciprocal microwave devices based on magnetic nanowires," *Appl. Phys. Lett.*, vol. 94, no. 20, May 2009, Art. no. 202505.
- [7] W. Zhou, J. Um, B. Stadler, and R. Franklin, "Design of self-biased coplanar circulator with ferromagnetic nanowires," in *Proc. IEEE Radio Wireless Symp. (RWS)*, Jan. 2018, pp. 240–242.
- [8] M. Sharma and B. K. Kuanr, "Microwave devices based on template-assisted NiFe nanowires: Fabrication and characterization," J. Phys. D, Appl. Phys., vol. 53, no. 6, Feb. 2020, Art. no. 065001.

- [9] L. Carignan, C. Caloz, and D. Menard, "Dual-band integrated self-biased edge-mode isolator based on the double ferromagnetic resonance of a bistable nanowire substrate," in *IEEE MTT-S Int. Microw. Symp. Dig.*, Anaheim, CA, USA, May 2010, pp. 1336–1339.
- [10] S. S. Kalarickal *et al.*, "Ferromagnetic resonance linewidth in metallic thin films: Comparison of measurement methods," *J. Appl. Phys.*, vol. 99, no. 9, May 2006, Art. no. 093909.
- [11] C. Kittel, "On the theory of ferromagnetic resonance absorption," Phys. Rev., vol. 73, no. 2, pp. 155–161, Jan. 1948.
- [12] W. Zhou et al., "Development of a biolabeling system using ferromagnetic nanowires," *IEEE J. Electromagn.*, RF Microw. Med. Biol., vol. 3, no. 2, pp. 134–142, Jun. 2019.
- [13] Y. Zhang, J. Um, B. Stadler, and R. Franklin, "Signal enhancement for ferromagnetic resonance measurement of magnetic nanowire array," in *Proc. IEEE Int. Symp. Antennas Propag.* USNC-URSI Radio Sci. Meeting, Atlanta, GA, USA, Jul. 2019, pp. 1305–1306.
- [14] A. Encinas, M. Demand, L. Vila, L. Piraux, and I. Huynen, "Tunable remanent state resonance frequency in arrays of magnetic nanowires," *Appl. Phys. Lett.*, vol. 81, no. 11, pp. 2032–2034, Sep. 2002.
- [15] Y. Zhang, J. Um, W. Zhou, B. Stadler, and R. Franklin, "Magnetic nanowires for RF applications: Ferromagnetic resonance and permeability characterization," in *IEEE MTT-S Int. Microw. Symp. Dig.*, Boston, MA, USA, Jun. 2019, pp. 1100–1103.